Proceedings World Geothermal Congress 2015
Melbourne, Australia, 19-25 April 2015

Nonlinear Parameter Estimation Based on History Matching of Temperature Measurements for Single-Phase Liquid-Water Geothermal Reservoirs

Mustafa Onur and Yildiray Palabiyik

Department of Petroleum and Natural Gas Engineering, Istanbul Technical University, Maslak, Istanbul, Turkey

onur@itu.edu.tr, palabiyik@itu.edu.tr

Keywords: History Matching, Temperature Data, Analytical Solution, Single-Phase Liquid-Water Geothermal Reservoirs

ABSTRACT

In this study, the main objective is to investigate the use of temperature data through history matching for estimating the reservoir parameters related to fluid and heat flow. The investigation is conducted by using an analytical solution based on the modification of the analytical solution of Chekalyuk (1965) as a forward model to compute both transient pressure and temperature behaviors of a single-phase, liquid-water infinite-acting geothermal system. Our modification involves the incorporation of the skin factor into the original solution of Chekalyuk (1965) who did not consider the skin effects in temperature solution. Only, the constant-rate production tests were considered. Both the gradient based Levenberg-Marquardt and non-gradient Ensemble Kalman Filters (EnKF) have been considered as the non-linear parameter estimation methods. To simulate real cases, temperature data generated from the analytical solution were corrupted with normally distributed noise. The results show which of the reservoir parameters (e.g., skin, porosity, permeability, fluid and rock densities and heat capacities) can be reliably estimated from the sandface temperature transient data in the presence of noise, recorded during constant-rate drawdown tests. A comparison of the Levenberg-Marquardt and the EnKF in terms of estimation procedure and computational performance for the problem of interest is also provided.

1. INTRODUCTION

The reservoir characterization through integration of dynamic data such as pressure, rate, etc., through history matching has become commonplace throughout the petroleum and geothermal industries. Although temperature data are routinely recorded in well test applications, the use of temperature data in addition to pressure for estimating the parameters controlling the fluid and heat flow for the purpose of reservoir characterization has been ignored in the past. The temperature data for history matching has recently attracted the attention of various researchers. In the petroleum and geothermal literature, it has been shown that temperature in addition to pressure can be a good source of data for reservoir characterization by the use of simple both lumped-parameter and distributed-parameter (1D, 2D and 3D) flow models (Onur et al. 2008a, b; Sui et al. 2008a, b; Ramazanov et al. 2010; Duru and Horne 2010a, b).

To the best of the authors' knowledge, Onur et al. (2008a) were to first to investigate the use of temperature data together with pressure data in history matching for estimating reservoir parameters of fluid and heat flow or geothermal related flow problems. Their investigation was based on a non-isothermal lumped-parameter model capable of estimating both pressure and temperature responses of a single-phase liquid-dominated geothermal reservoir idealized as a single-closed or recharged tank. Their model is solely based on the convection and neglected the conduction. Then, using this lumped-parameter model as a forward model in a gradient based history-matching algorithm [the Levenberg-Marquardt method with the restricted step procedure as described by Fletcher (1972)], they showed that one could estimate reservoir parameters such as the bulk volume and porosity of reservoir confidently if the average reservoir temperature data along with average pressure data is used for the purpose of history-matching. In another work based on the same non-isothermal lumped-parameter model, Onur et al. (2008b) also showed that if the specific heat capacity and density of the reservoir rock, recharge coefficient, recharge source temperature are added to the unknown parameter set, then the parameter estimation problem based on history matching problem becomes ill-conditioned, but one could estimate the porosity and the bulk volume of the reservoir in confidence by history matching temperature and pressure data. Later, Tureyen et al. (2009) extended the non-isothermal lumped-parameter model of Onur et al. (2008b) to a more general non-isothermal model of multiple tanks and investigated the use of temperature data in history matching for estimation of reservoir parameters from such a non-isothermal forward model. The main conclusion of Tureyen et al. (2009) is that while pressure allows estimation for only the initial pressure, pore volume, and the recharge index, the additional temperature information allows estimation for other parameters, particularly for the bulk volumes and porosities of the reservoir and aquifers. Although both the Onur et al. (2008a) and Tureyen et al. (2009) models provide useful insights on understanding of information content of average reservoir temperature in terms of model parameter estimation; nonetheless, spatial changes in pressure and temperature cannot be modeled using such lumped-parameter models, and hence cannot be used to investigate the information content of the bottom-hole pressure and temperature at a well for parameter estimation purposes.

In petroleum engineering literature, a 2D (*r*-*z*) radial simulator modeling temperature response for the case of single-phase slightly compressible fluid flow in 2D stratified systems has been presented by Sui et al. (2008a). Sui et al. (2008a) have indicated that the wellbore temperature is sensitive to the radius and permeability of damage zone around the wellbore in stratified systems. In their work, although the developed energy balance equation contains the effects of Joule-Thomson and thermal expansion, pressure used in energy balance equation has been obtained from the mass balance equation that makes the assumptions of isothermal flow and slightly compressible fluid. This is the same assumption as the one used in Ramazanov et al. (2010) and Duru and Horne (2010a)'s studies. An algorithm for an inverse solution formulated as a non-linear least-squares regression problem to estimate permeability (region outside damage zone), porosity, radius and permeability of damage zone by history matching observed temperature and pressure data has been given by Sui et al. (2008b) as another study. The claim that the mentioned parameters could reliably be

estimated by history matching temperature data if noise in temperature measurements is not very high is the important result of this study. Besides, a transient, 1D radial model coupling the mass and energy balance equations to estimate the pressure and temperature responses of a system with the components oil, connate water and rock has been given by App (2010) who has shown the pressure and temperature responses in the reservoir because of Joule-Thomson expansion of fluids under non-isothermal conditions.

Duru and Horne (2010b) have realized another study about the information content of transient temperature data. An inverse solution of permeability and porosity distributions in reservoir has been presented by history matching to temperature data with the method of Ensemble Kalman Filter (EnKF) using a forward model based on a coupled numerical solution of mass and energy balance equations for a 3D (*x*-*y*-*z*) system. Duru and Horne (2010b) have indicated with this study that temperature data contain more information about porosity distribution than that of permeability distribution.

In this work, we consider a relatively simple problem; a fully-penetrating vertical well producing at a constant-rate under 1D radial non-isothermal flow in an infinite-acting single-phase liquid water geothermal reservoir for investigating the use of the temperature transients in history matching. Two different parameter estimation methods; gradient based Levenberg-Marquardt and non-gradient Ensemble Kalman Filters (EnKF), are used. For our investigation, the "simple" analytical solution of Chekalyuk (1965) as the forward model for computing pressure and temperature transients is used.

The paper is organized as follows: a brief description of the modified version of the Chekalyuk (1965) analytical solution, incorporating the skin effects near the wellbore, which is used as the forward model, is provided next, and then the details of the history-matching methods used for performing match of the observed pressure and temperature data are discussed. Finally, the applications for parameter estimation with the synthetic transient pressure and temperature data in the presence of noise are demonstrated.

2. ANALYTICAL SOLUTION

The forward model considered in this work is based on the modified version of the analytical solution of Chekalyuk (1965). Chekalyuk's original solution did not include the effect of skin factor (*S*) near wellbore due to stimulation and damage (see Earlougher's classical SPE monograph for the concept of skin factor; Earlougher 1977). In this work, we have modified the original Chekalyuk temperature solution to incorporate the skin factor. Later in this section, we check the validity of the pressure and temperature solutions computed from the analytical solution with and without skin effects with the corresponding solutions computed from a 2D (*r*-*z*) simulator developed by Palabiyik et al. (2013).

The analytical solution assumes 1D radial fluid and heat flow towards a fully-penetrating line-source vertical well of uniform thickness producing at constant-rate in an infinite acting reservoir with no-fluid and heat flow across its top and bottom boundaries. Only convective heat transfer for which the effects of Joule-Thomson and adiabatic expansions are included on temperature transients. The effect of conduction is neglected as it has usually not have a significant effect on temperature transients during production periods. The solution also assumes a single-phase flow of a slightly compressible fluid of constant viscosity and constant isothermal compressibility in an infinite-acting homogeneous reservoir. Chekalyuk (1965) decouples the diffusivity equation for pressure and convective heat flow equation for temperature by assuming that the coefficients in the diffusivity and heat flow equations are independent of pressure and temperature. The solution ignores the wellbore storage and non-isothermal thermal effects in the wellbore. Here, we modified the Chekalyuk (1965) equation to include the skin factor by simply treating it as a steady-state pressure drop and adding this pressure drop into the wellbore pressure solution with zero skin (i.e., no damage or no stimulation at the sandface).

Under the aforementioned assumptions, the Chekalyuk solution for the sandface temperature is given by:

$$T_w(t) = T^0 - \mu_{JT,w}\left[\Delta p_w(t) + \frac{q\mu_w}{4\pi kh}(1+\alpha)\,\mathrm{Ei}\left(-\frac{r_w^2}{4\eta t} - \zeta\right)\right] \tag{1}$$

where Ei(-x) is the exponential integral function given by

$$\mathrm{Ei}(-x) = \int_x^\infty \frac{e^{-u}}{u}du \tag{2}$$

and Δp is the bottom-hole pressure drop at the sandface and is given by:

$$\Delta p_w(t) = p^0 - p_w(t) = \frac{q\mu_w}{4\pi kh}\left[-\mathrm{Ei}\left(-\frac{r_w^2}{4\eta t}\right) + 2S\right] \tag{3}$$

Here, S is the skin factor, and η is the diffusivity constant:

$$\eta = \frac{k}{\phi c_t \mu_w} \tag{4}$$

The variables α and ζ in Eq. 1 are given by, respectively:

$$\alpha = \frac{\left(\mu_{JT,w} + \dfrac{1}{C_{p,w}\rho_w}\right)\phi}{\mu_{JT,w}}\left[\frac{C_{p,w}\rho_w}{\phi C_{p,w}\rho_w + (1-\phi)C_{p,s}\rho_s}\right] \tag{5}$$

and

$$\zeta = \frac{q}{4\pi h\eta}\left[\frac{C_{p,w}\rho_w}{\phi C_{p,w}\rho_w + (1-\phi)C_{p,s}\rho_s}\right] \tag{6}$$

In Eqs. 1-6, q is well's volumetric production flow rate (m^3/s), h is the formation thickness (m), S is the skin factor (dimensionless), $\mu_{JT,w}$ is the Joule-Thomson coefficient (K/Pa), μ_w is the fluid viscosity (Pa s), ϕ is porosity (fraction), k is the permeability (m^2), c_t is the total isothermal compressibility of the liquid-water and rock system ($c_t = c_r + c_w$, where c_r is the effective isothermal rock compressibility and c_w is the isothermal water compressibility), $C_{p,w}$ is the specific heat capacity of water (J kg/K), $C_{p,s}$ is the specific heat capacity of the solid rock (J kg/K), ρ_w is the density of the liquid-water (kg/m^3) and ρ_s is the density of the solid rock (kg/m^3). T^0 and p^0 are the initial reservoir temperature (K) and pressure (Pa).

Now, we check the agreement of the temperature and pressure solutions given by Eqs. 1 and 3 with the corresponding solutions computed from a 2D (r-z) numerical simulator developed by Palabiyik et al. (2013) for two different data sets. Both data sets are based on the same basic input data given in Table 1. The only difference between the two cases is that the value of the skin factor; S = 0 and S = 5). In the simulator, the effect of skin is incorporated through the use of the effective wellbore radius concept; i.e., $r_w' = r_w e^{-S}$, where r_w' is the effective wellbore radius. It is important to note that the numerical simulator is quite general in that it rigorously solves the mass and energy balances, treat rock and fluid properties as a function of both pressure and temperature, include the effects of Joule-Thomson expansion for the fluid and adiabatic expansions for fluid and rock and the conductive heat transfer on pressure and temperature transients. In Table 1, β_s is the isobaric thermal expansion coefficient of rock and set it to zero in the simulator because the analytical solutions (Eq. 1 and 3) do not consider the effects of isobaric thermal expansion on pressure and temperature transients. λ_t is the total system thermal conductivity and again, set it to zero in the simulator because Eqs. 1 and 3 do not consider the effects of conductive heat transfer both in the rock and fluid. Comparisons of pressure and temperature numerical and analytical solutions are shown in Figs. 1 and 2. The number of grid blocks used in the radial direction to simulate the pressure and temperature data from the simulator is 200. As can be seen from Fig. 1, we have perfect matches of the analytical pressure solutions with the numerical pressure solutions for both cases of skin factor. Although the matches of analytical temperature solutions for the corresponding numerical temperature solutions seem to be not good for both cases of the skin factor, however, the differences between the solutions are quite small and less than 0.01%. Note also that the late-time behaviors of both the numerical and analytical solutions are quite similar and exhibit the same linearly increasing trends with the logarithm of time as predicted by the analytical solution of Eq. 1. Hence, we can state that the agreement of the analytical pressure and temperature solutions with those of the numerical simulator are acceptable considering the fact that the numerical simulator rigorously solve the mass and thermal balance equations by accounting for the variations of the coefficients of the balance equations (e.g., density, specific heat of water, isobaric thermal expansion of the water with pressure and temperature, whereas the analytical solution treats those coefficients as constant.

Table 1: Input parameter used for comparison of the Chekalyuk (1965) solution.

Parameter	Value
q, m^3/s	0.0322
p^0, kPa	10000
T^0, K (^{0}C)	413.15 (140)
r_w, m	0.1
r_e, m	10000
h, m	100
ϕ	0.2
k , m^2 (md)	9.869×10^{-14} (100)
c_r, 1/kPa	2.9×10^{-7}
c_w, 1/kPa	5.8×10^{-7}
β_s, 1/K	0.0
$C_{p,s}$, J/kg-K	1000
$C_{p,w}$, J/kg-K	4255
ρ_s, kg/m^3	2650
ρ_w, kg/m^3	931.3
μ_w, Pa.s	1.9837×10^{-4}
λ_t, J/m-s-K	0.0
$\mu_{JT,w}$, K/Pa	-1.585×10^{-7}

Finally, it is worth noting that, as can be seen from Fig. 1, a semi-log plot of flowing bottom-hole pressure versus time for both cases of skin factor yields a well-defined straight line, as in the case of isothermal flow (Earlougher 1977). This indicates that one

can estimate permeability and skin accurately from semi-log straight line analysis based on the assumption that the fluid properties such as viscosity, isothermal compressibility of water, as constant with temperature. In another words, this indicates that non-isothermal effects at a constant-rate production do not cause significant changes in flowing bottom-hole temperature/pressure data. As can be clearly seen from the temperature data shown in Fig. 2, temperature changes are quite small for this case. Interestingly, a semi-log plot of flowing bottom-hole temperature versus time also yields a straight-line proportional to Joule-Thomson coefficient. The increase in temperature though small for the synthetic problem considered here is due to Joule-Thomson heating of water. The magnitude of the increase in the flowing bottom-hole (or sandface) temperature change depends on significantly on flow rate, permeability and porosity. For instance, decreasing permeability increases the magnitude of the temperature change over a time. Details can be found in a study conducted by Palabiyik et al. (2015). Although not presented here, the approximate equations for the flowing bottom-hole temperature and pressure can be derived from Eqs. 1 and 3 by replacing the exponential integral functions in Eqs. 1 and 3 by their logarithmic approximations; i.e., $-\mathrm{Ei}(-x) = -\ln(xe^{\gamma})$, where $\gamma = 0.577215$ and represents the Euler constant (Abramowitz and Stegun 1972). These equations indicate that a semi-log plot of sandface temperature data versus time should exhibit two semi-log straight lines; one at early times and the other at late times; as can be noticed on the temperature data computed from the analytical solution of Eq. 1 in Fig. 2. The slope of the late-time semi-log straight line may be used to compute the Joule-Thomson coefficient $\mu_{JT,w}$ if the permeability of the system is known or computed from semi-log analysis of pressure versus time data. The slope of the early-time semi-log straight line may be used to compute the constant α given by Eq. 5 provided the Joule-Thomson coefficient and permeability could be estimated from late-time semi-log analyses of pressure and temperature data. Of course, if the rock and fluid specific heat capacities and densities are known *a priori*, one could estimate porosity from the value of α estimated from the slope of the early-time semi-log line of the temperature data. If the rock and fluid specific heat capacities and densities are not known, it is apparent from Eqs. 1 and 3 that it is very difficult if not impossible to uniquely estimate these parameters from temperature transient data, as our results to be given in the section entitled "Synthetic Applications" also confirm this observation.

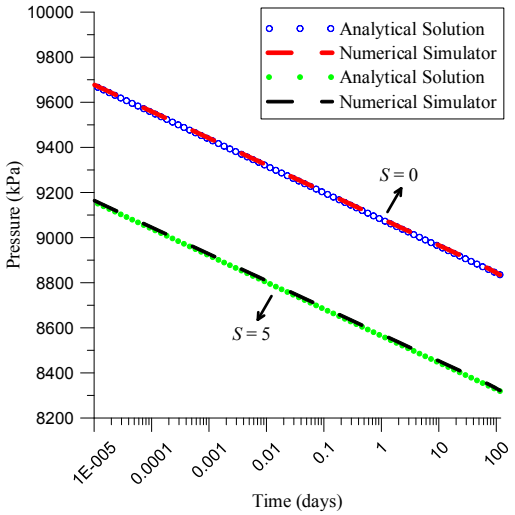

Figure 1: Comparison of modified Chekalyuk pressure solutions with those of a numerical simulator (Palabiyik et al. 2013).

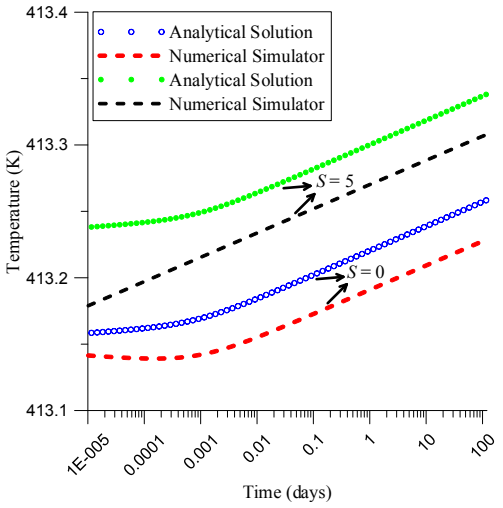

Figure 2: Comparison of modified Chekalyuk temperature solutions with those of a numerical simulator (Palabiyik et al. 2013).

3. HISTORY MATCHING METHODS

Here, a brief description of the history-matching methods considered in this study is given. As stated before, we consider both gradient and non-gradient methods for history matching temperature and/or pressure data. The gradient method used in this study is the Levenberg-Marquardt (L-M) method based on a restricted procedure as described by Fletcher (1987). It is a quite efficient method for over-determined problems (the number of model parameters to be estimated is far less than the number of observed/measured data to be history matched) as the one considered here. The other method is a non-gradient Ensemble-Kalman filter (EnKF). Although the use of EnKF is advantageous for underdetermined problems of parameter estimation; i.e., the number of model parameters are far more than the number of observed data and EnKF provides rigorous sampling of posterior parameter distribution for linear problems, here we investigate how it works for an over-determined nonlinear problem based on the analytical temperature solution considered here. In the following two subsections, some details of each parameter estimation method are given.

3.1 Gradient Based L-M Method

The gradient based L-M method is used to minimize a weighted least-squares objective function which is designed in a general way as to be able to match pressure or temperature or both data sets simultaneously:

$$O(\mathbf{m}) = \frac{1}{2} I_p \sum_{i=1}^{N_p} \left[w_{p,i} \left[\frac{p_{obs,i} - p_{cal}(\mathbf{m}, t_i^p)}{\sigma_p^2} \right] \right]^2 + \frac{1}{2} I_T \sum_{j=1}^{N_T} \left[w_{T,j} \left[\frac{T_{obs,j} - T_{cal}(\mathbf{m}, t_j^T)}{\sigma_T^2} \right] \right]^2 \quad (7)$$

The model parameter vector, **m**, in Eq. 7 can, in general, contain 13 model parameters as unknown as given by

$$\mathbf{m} = \left[k, h, \mu_w, S, \phi, c_t, C_{p,s}, C_{p,w}, \rho_s, \rho_w, \mu_{JT,w}, T^0, p^0\right]^T \tag{8}$$

Here, T is the transpose of the vector. The I_p and I_T terms in Eq. 7 are indicators which can only be either a "1" or a "0". These indicators are used for matching either pressure, temperature or both. T_{obs} and p_{obs} represent the observed (measured) temperature and pressure times t^T and t^p, respectively. T_{cal} and p_{cal} are the corresponding computed temperatures and pressures from the Chekalyuk pressure and temperature solutions given by Eqs. 1 and 3. N_p and N_T are the total number of data to match for pressure and temperature, respectively. σ_p and σ_T represent the standard deviations of the errors associated with the pressure data and the temperature data, respectively. $w_{p,i}$ and $w_{T,j}$ are the weights assigned to the pressure and temperature data, respectively. These weights are assigned by the user as 0 or a positive number. The gradient based Levenberg-Marquardt method based on a restricted procedure described by Fletcher (1987) is quite efficient to minimize Eq. 7. We have also constrained the parameters based on the procedure of Carvalho et al. (1992).

It should be noted that we have included almost all of the individual parameters appearing in Eqs. 1-6. However, we realize that it will be very difficult if not impossible to estimate uniquely each of these individual parameters. Instead, one may work with the following 10 grouped parameters to make the parameter estimation problem better well-posed, although we have not pursued this model parameter set in this study:

$$\mathbf{m} = \left[k / \mu_w, S, \phi, c_t, \mu_{JT,w}, (\rho_w C_{p,w}), (\rho C)_r, h, T^0, p^0\right] \tag{9}$$

Here, $(\rho C)_r$ is the ratio of thermal capacity of fluid to thermal capacity of the total system (note that the product of density and specific heat is referred to as the thermal capacity) defined by:

$$(\rho C)_r = \frac{C_{p,w}\rho_w}{\phi C_{p,w}\rho_w + (1-\phi)C_{p,s}\rho_s}. \tag{10}$$

3.2 Non-Gradient Based EnKF Method

EnKF is a Monte Carlo method where uncertainty is represented by an ensemble of realizations. The prediction of the uncertainty is performed by ensemble integration using the forward model (Evensen 2003). An overview of the applications of EnKF in the petroleum industry is given in Aanonsen et al. (2009). Our implementation of the EnKF in this work follows those of Zafari and Reynolds (2007) and Li et al. (2010). It should be noted that the EnKF is based on assumptions of the linear model, Gaussian distribution of the model parameters, and Gaussian errors in observed data. Although our model considered here is nonlinear, we would like to see the applicability of the EnKF for the nonlinear model considered here. Previously, Tureyen et al. (2007) applied the EnKF method for history-matching pressure data by the use of isothermal lumped-parameter models for single-phase liquid-water geothermal reservoirs. They showed that the EnKF can work for such non-linear models.

In the EnKF method, we define a state vector. Then, the method proceeds with a forecast step (stepping forward in time) and an assimilation step in which the state vector including the model parameters of the system are updated or corrected to honor the measured data. In our application, the initial ensemble is an ensemble of realizations of the prior probability distribution function of a particular uncertain parameter (e.g. permeability, porosity, etc.) generated by random fields.

For the problem considered here, we use the following EnKF update equation for the jth ensemble member at time t_r, where we have observed data (Li et al. 2010 and Morton et al. 2011):

$$\mathbf{y}_j^{r,u} = \mathbf{y}_j^{r,p} + \mathbf{C}_{Y^r,D^r}\left(\mathbf{C}_{D^r} + \mathbf{C}_{D^r,D^r}\right)^{-1}\left(\mathbf{d}_{uc,j}^r - \mathbf{d}_j^{r,p}\right), \tag{11}$$

for $j = 1,2,\ldots,N_e$. Here, N_e is the number of ensemble members. In Eq. 11, the superscripts $\boldsymbol{u}$ and $\boldsymbol{p}$ refer to updated and predicted quantities, respectively. $\mathbf{y}$ is the N_y-dimensional state vector at time t_r defined by

$$\mathbf{y}^r = \begin{bmatrix}\mathbf{m} \\ \mathbf{pT}^r\end{bmatrix}, \tag{12}$$

where $\mathbf{m}$ represents the N_m-dimensional vector of model parameters (see Eq. 8); where N_m represents the total number of unknown model parameters, and $\mathbf{pT}$ represent N_{pT}-dimensional vector of wellbore pressures and/or temperatures computed from the analytical pressure and temperature solutions of Chekalyuk (see Eqs. 1-6); where N_{pT} is the total number of computed pressures and/or temperatures. Note that $N_y = N_{pT} + N_m$. $\mathbf{d}_{uc,j}^r$ is the N_r-dimension vector of perturbed observed data, generated by adding Gaussian noise of mean zero and covariance $\mathbf{C}_{D^r}$ to the observed data at time t_r, and $\mathbf{d}_j^{r,p}$ is the N_r-dimensional vector of observed data at the data assimilation time t_r. N_r is the number of observed data to be used in assimilation time t_r. In our formulation, we expressed the observed data to be $p_w(t_r)$ and/or $T_w(t_r)$ measured at time t_r with a known, uncorrelated Gaussian, error variance of $\sigma^2_{wm}(t_r)$. So, the matrix $\mathbf{C}_{D^r}$ is a diagonal matrix. In Eq. 11, the covariance matrices $\mathbf{C}_{Y^r,D^r}$ and $\mathbf{C}_{D^r,D^r}$ are computed from the ensemble predictions by:

$$\mathbf{C}_{Y^r,D^r} = \frac{1}{(N_e-1)}\sum_{j=1}^{N_e}\left(\mathbf{y}_j^{r,u} - \bar{\mathbf{y}}^{r,p}\right)\left(\mathbf{d}_j^{r,p} - \bar{\mathbf{d}}^{r,p}\right)^T \tag{13}$$

and

$$\mathbf{C}_{D^r,D^r} = \frac{1}{(N_e-1)}\sum_{j=1}^{N_e}\left(\mathbf{d}_j^{r,p} - \bar{\mathbf{d}}^{r,p}\right)\left(\mathbf{d}_j^{r,p} - \bar{\mathbf{d}}^{r,p}\right)^T \tag{14}$$

where $\bar{\mathbf{d}}^{r,p}$ and $\bar{\mathbf{y}}^{r,p}$ represent the ensemble averages of the predicted data and state vectors, computed from:

$$\mathbf{d}_j^{r,p} = \frac{1}{N_e}\sum_{j=1}^{N_e}\mathbf{d}_j^{r,p}, \tag{15}$$

and

$$\bar{\mathbf{y}}^{r,p} = \frac{1}{N_e}\sum_{j=1}^{N_e}\mathbf{y}_j^{r,p}, \tag{16}$$

Note that $\mathbf{C}_{Y^r,D^r}$ is an $N_y \times N_r$ symmetric matrix, and $\mathbf{C}_{D^r,D^r}$ is an $N_y \times N_r$ matrix. The nice feature of this EnKF implementation is that these covariance matrices do not need to explicitly computed or stored. Further details of the EnKF method can be found in Evensen (2003), Aanonsen et al. (2009), and Li et al. (2010).

4. SYNTHETIC APPLICATIONS

Here, the applications for parameter estimation with the synthetic transient pressure and temperature data in the presence of noise are demonstrated. First, we simulate pressure and temperature data from Eqs. 1-6 for a constant-rate drawdown test of duration 120 days. The mass flow rate is 30 kg/s which corresponds to approximately 0.0322 m^3/s at the conditions of initial pressure and temperature. All other input data used to simulate this drawdown test data are as given in Table 1. We corrupted each simulated pressure and temperature data set by using normal random errors with different standard deviations [pressure and temperature containing errors of standard deviations of σ_p = 5000 Pa (= 0.05 bar = 0.725 psi) and σ_T = 0.002 K (= 0.002°C), respectively] and based the parameter estimation (i.e., nonlinear regression analysis) on these noisy pressure and temperature data sets. Shown in Figs. 3 and 4 are the semi-log plots of noisy pressure and temperature data used for nonlinear parameter estimation. In applications, we assume that we know or could estimate the variances (or std. deviation) of errors in pressure and temperature data to be used in the L-M and EnKF methods.

As plane radial flow (or infinite-acting radial fow) should apply for this synthetic data set, a semi-log plot of pressure vs. time data as shown in Fig. 3 yields a straight line with the slope from which the permeability value can be computed provided that the fluid viscosity and the thickness are known and with the intercept from which skin factor can be computed provided that porosity and the total isothermal compressibility is known (Earlougher 1977). Semi-log analysis of the data yielded $k = 9.861\times10^{-14}$ m^2 and S = 0.023, assuming that the porosity and the total system isothermal compressibility (c_t) are known *a priori*. The values of k and S estimated from the semi-log analysis are in very good agreement with the true (input) values (see Table 1). So, for this synthetic test case, bottom-hole pressure data provide very good estimates of k and S. Our results (not shown here) based on the nonlinear regression analysis of only pressure data by using both the L-M method and EnKF also confirm that history matching flowing bottom-hole pressure data yield reliable (confident) estimates of k and S if other input parameters such as porosity (ϕ), viscosity (μ_w) of the fluid and the total system isothermal compressibility (c_t) are known *a priori*. In the applications, we kept skin factor as known at its input value of zero, as one can obtain its value from semi-log analysis of pressure data accurately.

Next we history matched only the bottom-hole flowing temperature by using the gradient based L-M method to estimate five parameters; namely, ϕ, k, $C_{p,s}$, $C_{p,w}$ and $\mu_{JT,w}$. The values of the estimated parameters from this application along with 95% confidence intervals (which are given in ±) of the estimated parameters are given in Table 2. Although the temperature match obtained with the model temperature is not shown here, the match was quite acceptable with a root-mean-square (RMS) value equal to 2.0386×10^{-3} K, which is very close to the input value of standard deviation of errors used to corrupt the temperature data.

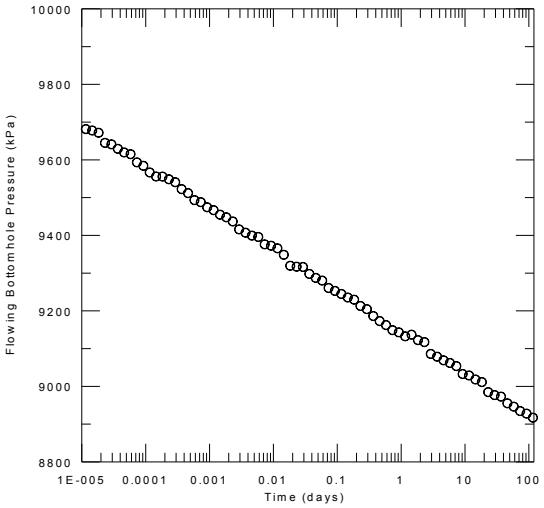

Figure 3: Noisy bottom-hole pressure data for synthetic drawdown test.

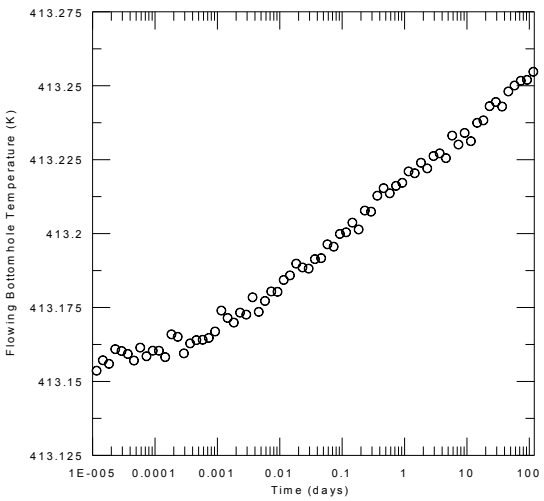

Figure 4: Noisy bottom-hole temperature data for synthetic drawdown test.

It is clear that only the value of permeability is confidently estimated. Although the estimated values of the other four parameters (ϕ, $C_{p,s}$, $C_{p,w}$ and $\mu_{JT,w}$) are close to the true, unknown input values, their confidence interval are quite high, which indicates that the

uncertainty in these estimated parameters are large. This may be due to small sensitivity of the temperature to these parameters and/or due to correlation among these parameters.

Next, we history matched both pressure and temperature data simultaneously to estimate the same five parameters, ϕ, k, $C_{p,s}$, $C_{p,w}$ and $\mu_{JT,w}$ by using the L-M method. The values of the estimated parameters from this application along with 95% confidence intervals (which are given in ±) of the estimated parameters are given in Table 3. Although not shown here both temperature and pressure matches obtained with the corresponding model data are quite acceptable and the values of RMS for pressure and temperature are RMS= 2.054×10^{-3} K (for temperature) and RMS= 5.523×10^{3} Pa (for pressure). Again these RMS values are very close to the input standard deviations of errors used to corrupt pressure and temperature data. Comparing the results given in Table 2 and 3, we can state that using both pressure and temperature data in history matching improves estimation and confidence especially for permeability and porosity. However, the confidence intervals are still quite large for the three thermal parameters; namely, $C_{p,s}$, $C_{p,w}$ and $\mu_{JT,w}$,. This is most likely due to high correlation among these parameters (see Eqs. 5 and 6).

Table 2: Estimated model parameters by history matching only temperature data; the L-M method.

Model Parameter	(Unknown) True Value	Initial Guesses	Estimated by history matching
ϕ, fraction	0.2	0.3	$0.131\pm2.03\times10^{4}$
k, m^2	9.869×10^{-14}	7.869×10^{-14}	$9.192\times10^{-14}\pm2.85\times10^{-8}$
$C_{p,s}$, J/kg-K	1000	1250	$998.10\pm1.3\text{x}10^{8}$
$C_{p,w}$, J/kg-K	4255	4300	$5276.97\pm2.0\text{x}10^{8}$
$\mu_{JT,w}$, K/Pa	-1.585×10^{-7}	-1.885×10^{-7}	$-1.494\times10^{-7}\pm6.5\text{x}10^{8}$
RMS = 2.0386×10^{-3} K			

Table 3: Estimated model parameters by history matching both pressure and temperature data; the L-M method.

Model Parameter	(Unknown) True Value	Initial Guesses	Estimated by history matching
ϕ, fraction	0.2	0.3	$0.189\pm1.12\times10^{-2}$
k, m^2	9.869×10^{-14}	7.869×10^{-14}	$9.899\times10^{-14}\pm4.1\times10^{-16}$
$C_{p,s}$, J/kg-K	1000	1250	$1017.2\pm1.02\text{x}10^{14}$
$C_{p,w}$, J/kg-K	4255	4300	$4289.3\pm4.4\text{x}10^{14}$
$\mu_{JT,w}$, K/Pa	-1.585×10^{-7}	-1.885×10^{-7}	$-1.623\times10^{-7}\pm6.5\text{x}10^{8}$
RMS = 2.0386×10^{-3} K (for temperature) and RMS= 5.523×10^{3} Pa (for pressure)			

Next, we history matched both pressure and temperature data by using EnKF method. As mentioned before, in EnKF method, we have to start with a number of model parameter realizations and a same number of unconditional realizations of the observed data. Here, we present our results only pertinent to a case where the number of realizations used is 100. The types of distributions and their corresponding parameters (mean and std. dev.) used for generating the unconditional realizations of the model parameters are given in Table 4.

Table 4: Assumed distributions of the model parameters for the EnKF method.

Model Parameter	Mean	Standard Deviation	Distribution Type
ϕ, fraction	0.2	5×10^{-2}	log-normal
k, m^2	9.869×10^{-14}	9.869×10^{-14}	log-normal
$C_{p,s}$, J/kg-K	1000	500	log-normal
$C_{p,w}$, J/kg-K	4255	2000	log-normal
$\mu_{JT,w}$, K/Pa	-1.585×10^{-7}	-1.0×10^{-8}	normal

Figures 5 and 6 show the computed model responses from initial ensembles for pressure and temperature data, respectively. As can be seen from Figures 5 and 6, bottom-hole pressure and temperature data predicted by using 100 initial ensembles of the model parameters are quite different from the observed data (shown as data points). Figures 7 and 8 show the history matched pressure and temperature responses, respectively, after updating each initial ensemble of the model parameters by the EnKF procedure. The results are acceptable because the ensemble means of 100 realizations of model parameters conditioned (or optimized) by history matching to observed data are close to the true unknown values (see Table 5). Furthermore, the computed ensemble means of

bottom-hole pressure and temperature data with each of 100 conditioned realizations of model parameters from $t = 0$ to the last time step of the observed data exhibit an excellent agreement with bottom-hole pressure and temperature curves which do not contain error. Moreover, from $t = 0$ to the last time step of the observed data, standard deviations between bottom-hole pressure and temperature data containing error and the ensemble means of bottom-hole pressure and temperature data computed is 5075.19 Pa and 0.0021 K for pressure and temperature, respectively. These values are in an excellent agreement with the standard deviations (5000 Pa for pressure and 0.002 K for temperature) of random errors used to corrupt the simulated bottom-hole pressure and temperature data without error (or noise).

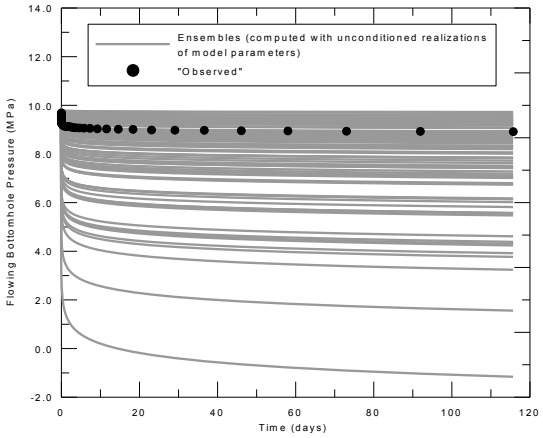

Figure 5: Bottom-hole pressure data computed from 100 unconditioned realizations of model parameters.

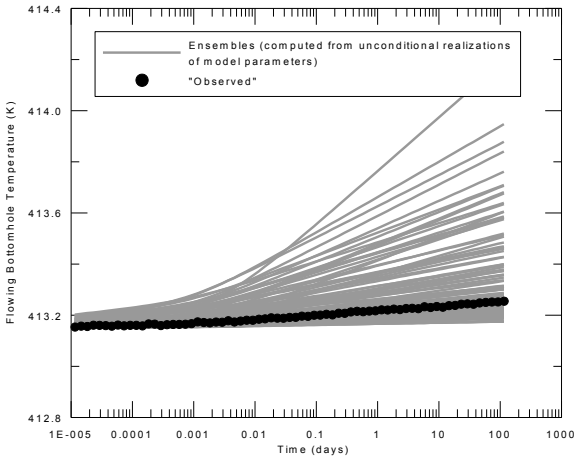

Figure 6: Bottom-hole temperature data computed from 100 unconditioned realizations of model parameters.

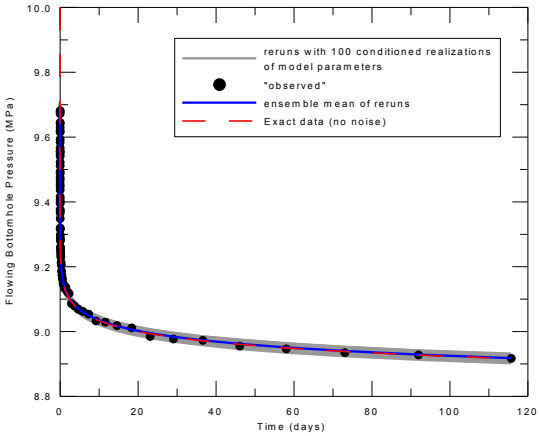

Figure 7: Bottom-hole pressure curves computed by the model starting from $t = 0$ for 100 conditioned realizations of model parameters.

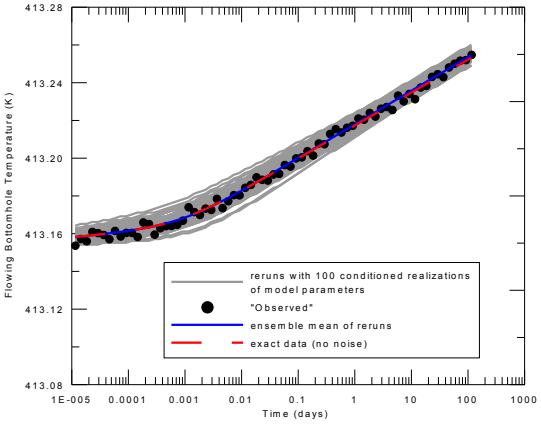

Figure 8: Bottom-hole temperature curves computed by the model starting from $t = 0$ for 100 conditioned realizations of model parameters

The values of the estimated model parameters with their estimated mean and std. dev. before and after the EnKF procedure method in comparison with the true (unknown) values of the model parameters are given in Table 5. The σ values given in the 2nd and 3rd columns in Table 5 represent the standard deviations (uncertainties) of the ensemble of each model parameter before and after history matching by EnKF. Before history-matching to measured data, as expected, the standard deviations of model parameters are high (see the 2nd column in Table 5). Uncertainties of model parameters are expected to decrease by history matching to measured pressure and temperature data. If σ values given for model parameters in the 3rd column in Table 5 are inspected, we see that the standard deviations of ensembles of model parameters conditioned by history matching to pressure and temperature data decreases in comparison with the standard deviations of the unconditioned model parameter ensembles. This is an expected and desired situation. However, reduction in the standard deviation of errors is parameter dependent; in other words, reduction may be significant for some parameters, while reduction may not be significant for other parameters. It is clear from Table 5 that the largest reduction in standard deviation is observed for permeability (in comparison with the standard deviation of the ensemble unconditioned). As can be seen from Table 5, history matching bottom-hole pressure and temperature data by the EnKF method reduces the standard deviation of ensemble of permeability conditioned by factor of 80. Indeed, this result is in agreement with the results obtained from the L-M method. Moreover, permeability is the parameter that has the smallest 95% confidence interval among the model parameters optimized by history matching with the L-M method (see Table 3).

Figures 9-11 show the comparisons of changes of posterior ensembles (100 realizations) pertinent to permeability, porosity and Joule-Thomson coefficient with their true values before and after history matching (conditioning), respectively. For instance, as can be seen from Fig. 9, each of 100 realizations is very close to true value of permeability after history matching. This is because bottom-hole pressure and temperature data show large sensitivity to permeability in comparison with the other model parameters. As to the other parameters, it is observed that the standard deviations of the parameters (ϕ, $C_{p,s}$, $C_{p,w}$, and $\mu_{JT,w}$) by the EnKF procedure decrease in comparison with those of their prior standard deviations. However, this decrease is not as much as in the standard deviation of the permeability (see Figures 9-11 and Table 5).

Table 5: Values and statistics of the estimated parameters from the EnKF method.

Model Parameter	(Unknown) True Value	Mean (and Std. Deviation) of Initial Ensembles	Mean (and Std. Deviation) of Ensembles Assimilated by EnKF
ϕ, fraction	0.2	0.210 (σ= 0.05)	0.212 (σ= 0.04)
k, m^2	9.869×10^{-14}	9.823×10^{-14} (σ=8.454×10^{-14})	9.867×10^{-14} (σ= 1.043×10^{-15})
$C_{p,s}$, J/kg-K	1000	966.9 (σ= 455.7)	878.7 (σ= 319.2)
$C_{p,w}$, J/kg-K	4255	3808.2 (σ=1968.6)	3513.0 (σ=1409.2)
$\mu_{JT,w}$, K/Pa	-1.585×10^{-7}	-1.576×10^{-7} (σ=1.03×10^{-8})	-1.618×10^{-7} (σ= 7.416×10^{-9})

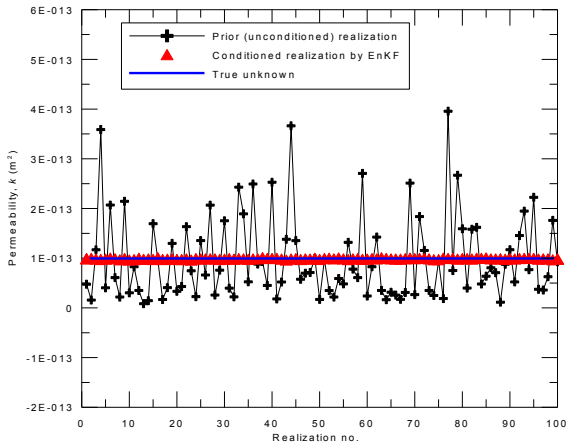

Figure 9: Comparison of unconditioned (prior) and conditioned ensemble realizations of permeability by EnkF method.

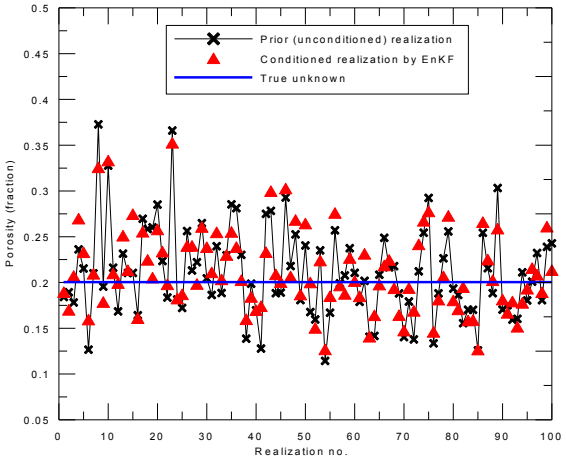

Figure 10: Comparison of unconditioned (prior) and conditioned ensemble realizations of porosity by EnKF method.

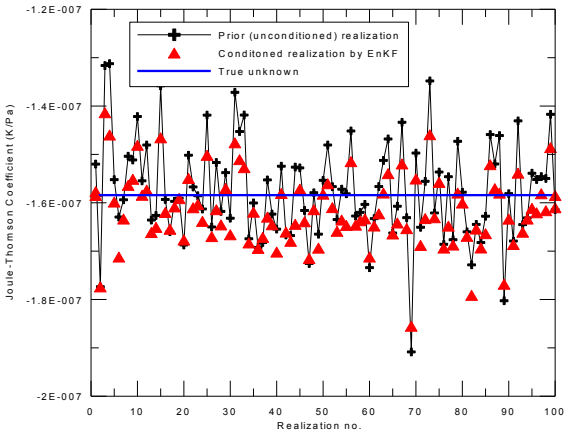

Figure 11: Comparisons of unconditioned (prior) and conditioned ensemble realizations of Joule-Thomson coefficient by EnKF method.

As to the computational efficiency of the gradient based L-M method and the non-gradient EnKF method, our results show that both methods are quite fast for this simple over-determined (model with five unknown model parameters) case studied here, though the EnKF requires a slightly more computation time. For the set of 100 realizations of the five unknown model parameters, the EnKF method only requires a few seconds for completion. Although we have not yet pursued, we think that the real advantage of the EnKF over the gradient based methods will be for the underdetermined parameter estimation problems based on the numerical models where each grid-block rock/fluid property is treated as unknown as pursued by Duru and Horne (2010b).

5. CONCLUSIONS

The main conclusions of this work can be stated as follows:

i. Based on the modified analytical solution of the Chekalyuk (1965), it is shown that the sandface temperature data during production from a vertical well at a constant-rate from an infinite acting reservoir exhibit a semi-log straight line at late times. This slope is proportional to the product of the permeability and the Joule-Thomson coefficient. The intercept of this straight line contain information about the skin factor and the specific heat capacities of the rock and fluid. However, a unique estimation of the individual values of permeability, porosity, skin, Joule-Thomson coefficient, specific heat capacities from temperature data alone in the presence of noise seems to be very difficult if not impossible due to strong correlation among the model parameters.

ii. As the pressure data for the well/reservoir model considered in this study should exhibit a semi-log straight line from which the permeability and skin factor can be reliably determined, hence, using pressure data with the temperature data in history matching improves the parameter estimation problem and allows one to estimate porosity and the Joule-Thomson coefficient confidently provided that the specific heat capacities and densities are assumed to be known *a priori*.

iii. It is observed that for the simple over-determined case studied here, both gradient-based L-M and EnKF methods are computationally efficient to use to history match pressure and temperature data and both methods give very similar results although the L-M method yields closer estimations to the true values of the model parameters.

iv. For the synthetic case study considered here, both optimization methods show that permeability, porosity, and the Joule-Thomson coefficient can be determined more reliably from pressure and temperature data in contrast to the other model parameters such as the specific heat capacities of rock and fluid properties if observed data contain error.

ACKNOWLEDGEMENTS

We would like to thank the Scientific and Technological Research Council of Turkey (TUBITAK, Project No: 110M482) and the Unit of ITU (Istanbul Technical University) Scientific Research Projects for the supports that they supply to finance this work.

REFERENCES

App, J.F.: Nonisothermal and Productivity Behavior of High Pressure Reservoirs, *SPE Journal*, **15**, (2010), 50-63.

Aanonsen, S. I., Noevdal, G., Oliver, D. S., Reynolds, A. C., and Valles, B.: The Ensemble Kalman filter in reservoir engineering - a review. *SPE Journal,* September, (2009), 393-412.

Abramowitz, M. and Stegun, I.A.: *Handbook of Mathematical Functions with Formulas, Graphs, and Mathematical Tables*, Tenth Editing, U.S. Department of Commerce, National Bureau of Standards, Washington (1972), 229.

Carvalho, R.S., Redner, R.A., Thompson, L.G., and Reynolds, A.C.: Robust Procedures for Parameter Estimation by Automated Type-Curve Matching, paper SPE No. 24732, SPE Annual Technical Conference and Exhibition, Washington, D.C (1992).

Chekalyuk, E.B., *Thermodynamics of Oil Formation,* (in Russian), Nedra, Moscow (1965).

Duru, O.O., and Horne, R.N.: Modelling Reservoir Temperature Transients and Reservoir-Parameter Estimation Constrained to the Model, *SPE Reservoir Evaluation & Engineering*, **13**, (2010a), 873-883.

Duru, O.O., and Horne, R.N.: Joint Inversion of Temperature and Pressure Measurements for Estimation of Permeability and Porosity Fields, paper SPE No. 134290, SPE Annual Technical Conference and Exhibition, Florence (2010b).

Duru, O.O., and Horne, R.N.: Combined Temperature and Pressure Data Interpretation: Applications to Characterization of Near-Wellbore Reservoir Structures, paper SPE No. 146614, SPE Annual Technical Conference and Exhibition, Denver, Colorado (2011).

Earlougher, R.C. Jr.: *Advances in Well Test Analysis*, Monograph Series No. 5, SPE, Dallas, TX (1977).

Evensen, G.: The Ensemble Kalman filter: Theoretical formulation and practical implementation. *Ocean Dynamics*, **53**, (2003) 343–367.

Fletcher, R.: *Practical Methods of Optimization*, John Wiley and Sons, Inc., New York (1989), 101.

Li, G., Han, M., Banerjee, R., and Reynolds, A.C.: Integration of well-test pressure data into heterogeneous geological reservoir models. *SPE Reservoir Evaluation and Engineering,* June, (2010), 496-508.

Morton, K.L., Booth, R.J., Onur, M., and Kuchuk, F.J.: Grid-Based Inversion Methods for Spatial Feature Identification and Parameter Estimation from Pressure Transient Tests, paper SPE 142996, SPE EUROPEC/EAGE Annual Technical Conference and Exhibition, Vienna, Austria (2011).

Onur, M., Sarak, H., Tureyen, O.I., Cinar, M., and Satman, A.: A New Non-Isothermal Lumped Parameter Model for Low Temperature, Liquid Dominated Geothermal Reservoirs and its Applications, *Proceedings*, 33rd Workshop on Geothermal Reservoir Engineering, Stanford University, Stanford, CA (2008a).

Onur, M., Sarak, H., Tureyen, O.I., Cinar, M., Satman, A., and Korkmaz, E.D: Modeling of Fluid and Heat Production Behavior of Low Temperature Geothermal Reservoirs by Lumped-Parameter Models, unpublished project report, TÜBİTAK project No. 105M018, (in Turkish), Ankara, Turkey, (2008b).

Palabiyik, Y., Tureyen, O.I., Onur, M., and Deniz, M.: A Study on Pressure and Temperature Behaviors of Geothermal Wells in Single-Phase Liquid Reservoirs, *Proceedings*, 38th Workshop on Geothermal Reservoir Engineering, Stanford University, Stanford, CA (2013).

Palabiyik, Y., Tureyen, O.I., and Onur, M.: Pressure and Temperature Behaviors of Single-Phase Liquid Water Geothermal Reservoirs Under Various Production/Injection Schemes, *Proceedings*, World Geothermal Congress, Melbourne, Australia, (2015).

Ramazanov, A.S., Valiullin, R.A., Sadretdinov A.A., Shako, V.V., Pimenov, V.P., Fedorov, V.N., and Belov, K.V.: Thermal Modeling for Characterization of Near Wellbore Zone and Zonal Allocation, paper SPE No. 136256, SPE Russian Oil and Gas Technical Conference and Exhibition, Moscow (2010).

Sui, W., Zhu, D., Hill, A.D., and Ehlig-Economides, C.: Model for Transient Temperature and Pressure Behavior in Commingled Vertical Wells, SPE Russian Oil and Gas Technical Conference and Exhibition, Moscow (2008a).

Sui, W., Zhu, D., Hill, A.D., and Ehlig-Economides, C.: Determining Multilayer Formation Properties from Transient Temperature and Pressure Measurements, paper SPE No. 116270, SPE Annual Technical Conference and Exhibition, Denver, Colorado (2008b).

Tureyen, O.I., Onur, M., and Sarak, H.: Assessing Uncertainty in Future Pressure Changes Predicted by Lumped Parameter Models: A Field Application, *Proceedings*, 32nd Workshop on Geothermal Reservoir Engineering, Stanford University, Stanford, CA (2007).

Tureyen, O.I., Onur, M., and Sarak, H.: A Generalized Non-Isothermal Lumped Parameter Model for Liquid Dominated Geothermal Reservoirs, *Proceedings*, 34th Workshop on Geothermal Reservoir Engineering, Stanford University, Stanford, CA (2009).

Zafari, M., and Reynolds, A.C.: Assessing the uncertainty in reservoir description and performance predictions with the ensemble Kalman filter. *SPE Journal,* September, (2007), 382-391.